

Feature article

Flash Graphene: a Sustainable Prospect for Electrocatalysis

Ivo Bardarov^{1,2}, Desislava Yordanova Apostolova¹, Maris Minna Mathew¹, Miha Nosan¹, Pedro Farinazzo Bergamo Dias Martins^{1,2} and Bostjan Genorio^{1*}

¹ University of Ljubljana, Faculty of Chemistry and Chemical Technology, Večna pot 113, SI-1000 Ljubljana, Slovenia

² National Institute of Chemistry, Department of Materials Chemistry, D10, Hajdrihova 19, SI-1000 Ljubljana, Slovenia

* Corresponding author: E-mail: bostjan.genorio@fkkt.uni-lj.si

Received: 05-07-2024

Abstract

The increasing demand for sustainable and efficient energy conversion technologies requires ongoing exploration of new materials and methods. Flash Joule Heating (FJH) emerges as a promising technique for large-scale graphene production, boasting advantages over conventional methods. FJH rapidly heats carbon-based precursors to extreme temperatures using high electric currents, forming flash graphene upon rapid cooling. This approach offers rapid processing, high throughput, and can utilize diverse carbon sources, including biomass and waste, making it sustainable and cost-effective. Moreover, it generates minimal waste and yields flash graphene with enhanced conductivity, crucial for energy applications. FJH's scalability, versatility, and efficiency position it as a key method for commercializing graphene across industries, particularly in energy conversion. This review comprehensively discusses FJH synthesis principles, emphasizing efficiency, scalability, and sustainability. Additionally, it analyzes recent advancements in flash graphene-based electrocatalysts, exploring their impact on renewable energy and sustainable electrocatalysis. Challenges and opportunities are addressed, outlining future research directions. Continued advancements hold immense potential to revolutionize graphene production and integrate it into next-generation energy systems, driving the transition towards cleaner energy solutions.

Keywords: Synthesis of graphene; Flash Joule heating; Flash graphene; Electrocatalysis

1. Introduction

Graphene, the foundational two-dimensional (2D) structure of all carbon's graphitic forms, has captured significant attention since its groundbreaking isolation in 2004 by Geim and Novoselov.¹ The significance of this achievement cannot be overstated and was duly recognized by the scientific community in 2010 when it earned the Nobel Prize in Physics.^{2,3} Prior to its isolation, graphene's remarkable properties remained largely unexplored due to its inherent binding to substrates (e.g., platinum single crystal surface).⁴ These properties encompass a broad spectrum, including exceptional attributes like high electron mobility (measuring at $2.5 \times 10^5 \text{ cm}^2 \text{ V}^{-1} \text{ s}^{-1}$)⁵ and extraordinary intrinsic mechanical properties (reaching 130 GPa),⁶ making graphene a suitable candidate for applications in completely unrelated fields e.g., electronics⁷ and cement⁸ technologies. Unsurprisingly, researchers spanning various fields of expertise have enthusiastically embarked on graphene experimentation, considering it a

prime candidate for replacing conventional materials in established applications. Moreover, its extensive array of astonishing properties has sparked optimism about the potential birth of disruptive technologies.⁷ Consequently, this surge of interest has given rise to a metaphorical "gold rush" directed towards diverse applications of graphene.⁹ Among those, the use of graphene and graphene-based materials for energy storage and conversion have shown considerable improvement over the past years.^{10–13} The aim of this work is to discuss the pros and cons of different graphene production methods in terms of scalability and sustainability, considering specifically its application as electrocatalysts for sustainable technologies. Focus is given to a relatively new synthesis method based on a process called flash Joule heating (FJH), how its versatility may open new doors for the easy tuning of graphene properties toward applications in energy-related technologies, and the potential for breaking into the market due to its simplicity and low-cost.

2. A Brief Introduction of the Main Methods for Graphene Production and Their Application in Electrocatalysis

For almost 20 years graphene-related research continues to be enthusiastic, and the quest for a method to produce defect-free flat carbon monolayers in large-scale persists. This journey, in turn, also gave rise to a rather upsetting fact at first glance; that graphene and graphene-based materials properties (physical, electronic, and optical) vary strongly with the method employed for their synthesis.¹⁴ Therefore, the production method used to pre-

pare any graphene-like material will ultimately enable or impede its final application. In fact, during this period, a so called “graphene family”¹⁵ of 2D carbon forms varying in terms of morphology, lateral dimensions, number of layers, different types and number of structural defects emerged. Despite the abundance of scientific publications focused on large-scale graphene production and manufacturing technologies, the practical implementation of graphene remains limited. To achieve industrial-scale applications, a mass production technique must not only yield the necessary quantities but also ensure consistent quality. Unfortunately, current graphene manufacturing methods continue to be either cost prohibitive or underde-

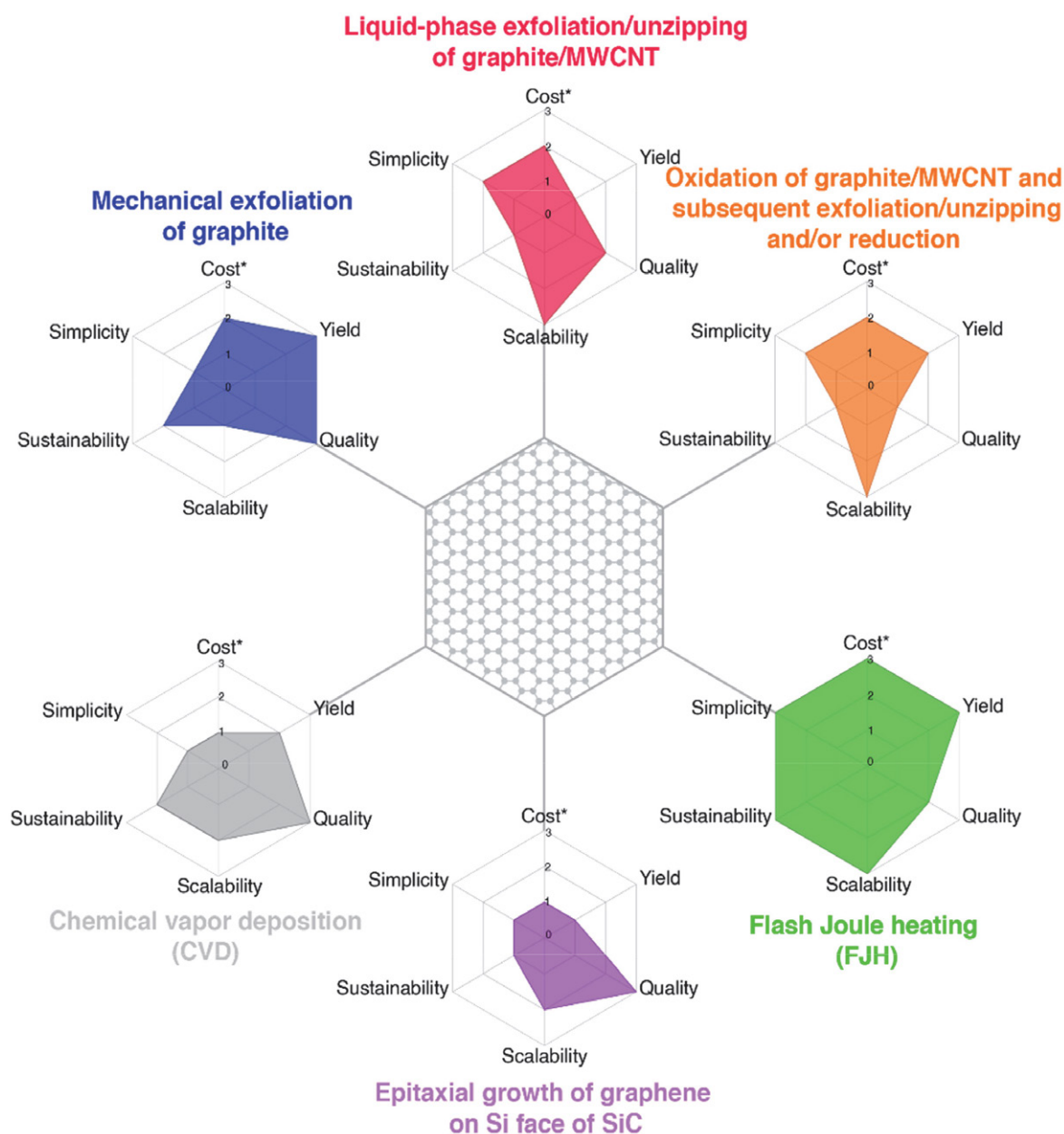


Figure 1. Schematic overview of common graphene production methods varying from top-down to bottom-up approaches. (*A low value represents a high-cost method).

veloped as new difficulties always emerge as the process is scaled from the research laboratory to the industry.^{16–28}

The main production methods of graphene and its derivative materials are shown in Figure 1. The produced graphene can be classified into two major characteristic groups, large area single layer graphene sheets and bulk graphene composed of graphene flakes having smaller lateral sizes. As it will be discussed later, bulk graphene is desirable for large-scale energy storage and conversion applications mainly due to its comparatively high surface area and relatively easy scalability.

2. 1. Mechanical Exfoliation

Mechanical exfoliation is a fundamental technique for producing graphene from graphite. This approach involves repeatedly cleaving a piece of highly ordered pyrolytic graphite (HOPG) with adhesive tape to obtain increasingly thin layers of graphene.¹ The pros of this method include its simplicity and the high quality of the graphene produced. It yields monolayer graphene with minimal defects and excellent electronic properties, making it suitable for various applications in electronics and nanotechnology. However, there are several cons associated with mechanical exfoliation. It is a time-consuming and labor-intensive process, limiting its scalability for large-scale production. Additionally, it is challenging to control the number of graphene layers produced, and it generates a substantial amount of waste material. As such, while mechanical exfoliation remains a crucial technique for research and fundamental studies of graphene, it may not be the most practical method for industrial scale production.²⁹

2. 2. Liquid-phase exfoliation (LPE)

Liquid-phase exfoliation (LPE) of graphite is widely employed by industries to produce graphene in large quantities. Its principle is based on weakening the interaction between graphite layers using non-aqueous solvents or aqueous solutions containing surfactants, followed by physical agitation or sonication to separate and disperse the graphene flakes. Due to incomplete delamination of the graphite precursor even after prolonged treatment, centrifugation is usually necessary to separate monolayer flakes from the bulk solution. Because of the presence of surfactants or organic solvents, a purification step is needed if the graphene flakes are to be used for energy storage and conversion applications. Moreover, LPE generates a lot of hazardous wastes, which renders it to be unsustainable for mass production of graphene.

2. 3. Oxidation with Successive Reduction

Another method heavily adopted by industry is the oxidation of graphite pellets, on which the graphite oxide

formed is ultrasonically exfoliated in aqueous solutions. The oxidation of graphite increases the inter-layer distance of individual sheets, hence facilitating its separation. The as-prepared graphene oxide (GO) flakes are isolated by centrifugation, followed by reduction to form reduced graphene oxide (rGO). The reduction process can be performed chemically or thermally; nevertheless, part of the product will always remain oxidized. One major drawback of this method is the introduction of structural defects in the rGO sheets, which may compromise the desired appealing properties of graphene. Like the LPE method, the production of rGO generates large quantities of harmful chemical waste, requiring extra-step(s) for its treatment before it can be discarded, which ultimately increases the overall cost of graphene production.

2. 4. Unzipping of Carbon Nanotubes

The top-down approach of graphene production through the unzipping of carbon nanotubes (CNTs) presents both advantages and drawbacks in the field of nanomaterial synthesis.³⁰ One key advantage is the inherent structural uniformity of carbon nanotubes, which facilitates the controlled production of graphene with well-defined characteristics.^{31,32} This approach allows for the tailoring of graphene sheets with specific dimensions and properties, offering versatility in applications ranging from electronics to energy storage.^{33–37} Moreover, the unzipping process enables the integration of functional groups onto the graphene surface, enhancing its compatibility with various matrices and facilitating the development of composite materials with tailored properties.^{38–40} Despite these advantages, drawbacks include the potential introduction of defects during the unzipping process, which can adversely impact the electrical and mechanical properties of the resulting graphene.^{31,38} Additionally, the scalability of this method may be limited, and the need for specialized equipment and precise control over reaction conditions poses challenges for large-scale production. For instance, the unzipping of carbon nanotubes (CNTs) through a solution-based oxidative treatment has been successfully demonstrated.⁴¹ This innovative method facilitates the longitudinal opening of multi-walled CNTs with an impressive yield approaching 100%, even on a large scale. However, it is noteworthy that this procedure is accompanied by certain limitations. Despite its efficiency, the resulting graphene ribbons exhibit a width surpassing 100 nm and are characterized by pronounced structural defects and oxidized sites, reminiscent of rGO. This outcome underscores the challenges associated with achieving precise control over the unzipping process, leading to the compromise of structural integrity and the introduction of undesirable chemical moieties. Consequently, while this approach presents a noteworthy step forward in the large-scale production of longitudinally opened CNTs, further refinement is essential to address the inherent issues relat-

ed to the dimensions and quality of the produced graphene materials. Advances in optimizing this methodology hold significant promise for unlocking the full potential of graphene-based structures across diverse scientific and technological applications.

2. 5. Chemical Vapor Deposition (CVD)

Chemical vapor deposition (CVD) is a prominent method for the large-scale production of graphene, offering several advantages and disadvantages in terms of cost, yield, reproducibility, and quality.^{42–48} It enables the synthesis of graphene on various substrates, mostly metals, such as copper or nickel surfaces, making it suitable for industrial applications.^{43,46,47,49–55} Moreover, CVD can yield high-quality graphene films with excellent electrical and mechanical properties, which are crucial for many advanced technologies.^{30,43,56–58} However, there are notable disadvantages associated with the CVD method. Cost can be a limiting factor, as it requires specialized equipment, precise control over reaction conditions, and the use of high temperatures and vacuum, making the initial setup and operation expensive. Additionally, the yield of high-quality graphene is greatly dependent on factors such as substrate quality and the need for post-processing steps to transfer graphene from the growth substrate. This can reduce the overall production efficiency and further increase costs. Reproducibility in CVD is another challenge, as slight variations in growth conditions can lead to differences in graphene quality and thickness. Achieving uniformity across large-scale production can be difficult, requiring tight process control.

Although the epitaxial growth of graphene on the Si crystal plane of silicon carbide (SiC) has emerged as a promising method to produce high-quality graphene, its distinct disadvantages, particularly in the context of large-scale production, inevitably restrict the use of graphene to fundamental research and restrict applications, such as electronic devices and high frequency transistors.⁵⁹ One significant advantage of this method is its ability to produce high-quality single-layer graphene directly on a technologically relevant substrate.^{42,60–63} The SiC lattice closely matches the graphene lattice, promoting epitaxial growth and reducing defects. This results in exceptional electronic quality, making it highly desirable for electronic and optoelectronic applications. Additionally, the method offers good reproducibility, as it relies on well-established semiconductor growth techniques.^{61–63} However, there are notable disadvantages to consider. First, the cost of SiC wafers and the epitaxial growth equipment can be relatively high, which poses a barrier to large-scale production. Second, while the quality of graphene produced through this method is exceptional, the process may not be as scalable as some other techniques. The growth rate may be limited, impacting overall yield and production speed. Furthermore, the requirement for spe-

cialized SiC substrates can limit versatility and increase costs.

2. 6. Polymerization from Organic Precursors

The organic synthesis of graphene is a bottom-up method based on the oxidative cyclodehydrogenation of oligophenylene and polyphenylene precursors to produce nanographene molecules and graphene nanoribbons (GNRs).^{30,64–70} The main advantage of this method is the possibility to create bandgap in the electronic structure of graphene and control its magnitude, which has enormous implications for application of graphene-based materials in electronic devices.^{71–81} For instance, by varying the width and edge termination of the GNRs, it is possible to tailor the magnitude of the bandgap with extreme precision, an essential step to design GNRs with accurate and reproducible electronic, optical, and magnetic properties for impending nanoelectronics, optoelectronics, and spintronics applications.^{29,82–86} However, the scalability of the organic synthesis of GNRs together with its transfer process remains challenging for practical application in devices.^{87,88}

2. 7. Graphene and Graphene-Based Materials as Passive Components for Electrocatalysis

Fuel cells are electrochemical devices that convert chemical energy directly into electrical energy. Graphene's high electrical conductivity, large surface area, and chemical stability make it an ideal candidate for various components in fuel cells. The use of graphene-based materials as catalyst supports, gas diffusion layers, and current collectors has shown remarkable improvements in the overall performance and durability of fuel cells.^{89–93} These advancements contribute to increased power density, faster reaction rates, and prolonged cell life. For instance, in a study conducted by Yoo et al., it was observed that sub-nano Pt clusters, when supported on graphene nanosheets (Pt/GNS), demonstrated superior CO tolerance during the hydrogen oxidation reaction (HOR) compared to Pt clusters dispersed on carbon black (Pt/CB).⁹⁴ Electrochemical characterization revealed that, under pure H₂ conditions, Pt/GNS, Pt/CB, and PtRu/CB exhibited comparable electrocatalytic activities for the HOR, notwithstanding the variation in the carbon material utilized. Notably, the Pt/GNS sustained a 52% activity level in the presence of H₂ and 500 parts per million (ppm) of CO, whereas the Pt/CB exhibited only 11% activity under the same conditions. Although the mechanism behind the improved CO tolerance for Pt/GNS remains unclear, these findings underscore the enhanced CO tolerance and high durability of Pt/GNS, positioning graphene-based electrocatalyst supports as promising candidates for improving the performance of fuel cells.

The oxygen reduction reaction (ORR) occurring at the cathodes of proton exchange membrane fuel cells (PEMFCs) is a crucial electrochemical process that significantly influences the overall efficiency of these energy conversion devices. Despite its importance, the slow kinetics associated with the ORR remains a major drawback, impeding the widespread deployment of practical fuel cells. The sluggish nature of the ORR can be primarily attributed to the complex four-electron transfer mechanism involved in reducing molecular oxygen to water. The intricate nature of this process, coupled with the inherently limited surface area of conventional cathode materials, results in substantial overpotential and hinders the rate of oxygen reduction. Kou et al. utilized functionalized graphene sheets (FGSs) as support for Pt nanoparticles as electrocatalyst for the ORR in acidic media.⁹⁵ Specifically, the FGSs were synthesized through the thermal expansion of graphite oxide, and Pt nanoparticles, featuring an average diameter of 2 nm, were homogeneously deposited onto FGSs utilizing impregnation methods. Comparative analysis revealed that Pt-FGS exhibited a superior electrochemical surface area and oxygen reduction activity, coupled with enhanced stability, in comparison to a commercially available catalyst (20% Pt supported on Vulcan XC-72 carbon). Complementary techniques such as transmission electron microscopy, X-ray photoelectron spectroscopy, and electrochemical characterization collectively indicate that the enhanced performance of Pt-FGS can be ascribed to the smaller particle size and reduced aggregation of Pt nanoparticles on the functionalized graphene sheets. This study highlights the significance of tailored catalyst-support systems in optimizing the electrocatalytic performance of oxygen reduction reactions for potential applications in energy conversion technologies.

A recent study about the influence of support's structure and chemistry on platinum-based electrocatalysts showed that graphene derivative (GD) support confers higher stability and activity during ORR compared to the commercial benchmark carbon black (CB) support.⁹⁶ Accelerated degradation testing, conducted utilizing a high-temperature liquid electrolyte disc electrode, revealed that reduced graphene oxide (rGO)-supported catalysts exhibited enhanced electrochemical stability in both electrochemically active surface area and mass activity retention compared to their CB-supported counterparts, including the commercially recognized benchmark from Umicore (Elyst Pt30 0690). X-ray photoelectron spectroscopy and Raman spectroscopy results suggested that the improved durability of the electrocatalyst is attributed to the increased content of sp^2 carbon and the reduction of structural defects in the rGO support. These alterations may induce a modified metal-support interaction, influencing the enhanced durability and performance of GD-supported catalysts. Furthermore, evaluation of high current density performance was conducted by measuring activity in a gas diffusion electrode half-cell. On average,

both electrocatalysts based on rGO exhibited superior kinetic performance and high current density, pertinent for industrial applications. Notably, the peak power density values of the rGO-supported materials in this study surpassed those reported in prior publications and exceeded the state-of-the-art commercial Pt-Co benchmark. This positions rGO-based materials as highly promising candidates for potential industrial applications as carbon-based catalyst supports, warranting further exploration in this direction.

Pavko et al. systematically assessed the durability of selected graphene derivatives (reduced graphene oxides, rGOs, and reduced graphene oxide nanoribbons, rGONRs) and carbon black (CB) employed as carbon supports for platinum-based ORR electrocatalysts.⁹⁷ Two distinct series of electrocatalysts, one based on PtCu and the other on Pt-Co nanoparticulate intermetallics, were uniformly dispersed on the specified carbon supports. Characterization through X-ray diffraction, transmission electron microscopy, and scanning electron microscopy indicated comparable metallic components in both series (PtCu and PtCo) of the composite samples, with the primary distinction lying in the nature of the carbon support - a critical consideration for investigating carbon support durability. In-depth X-ray photoelectron spectroscopy analysis affirmed substantial differences among the carbon supports in terms of total oxygen content, sp^2 carbon content, and the nature of oxygen functionalities. To assess carbon support durability, the authors conducted specialized electrochemical accelerated degradation tests (HT-ADTs), deliberately inducing carbon corrosion as the primary degradation mechanism. On average, electrocatalysts supported by rGO demonstrated superior electrochemical durability compared to their CB supported counterparts. Notably, the CB supported sample, despite exhibiting the lowest oxygen content, did not demonstrate the highest stability, suggesting that factors beyond total oxygen content significantly influence carbon support durability. Among these factors, the amount of sp^2 carbon and its corrosion stability emerged as crucial, specifically, higher sp^2 content correlated with increased durability of the carbon support. Finally, the paramount parameter influencing electrochemical durability was identified as the content of carboxyl functional groups; higher amounts of this functional group in the carbon support corresponded to lower electrochemical durability. These findings were corroborated by direct measurements of evolving CO_2 signals using an advanced *in-situ* electrochemical cell-mass spectrometry, which demonstrated carbon support degradation during potential cycling. The observed trend aligned with that of HT-ADTs, where the least stable catalyst exhibited the highest CO_2 signal, while the most stable catalyst exhibited the lowest, providing strong support for the results obtained from HT-ADTs. The knowledge gained can guide the development of more stable carbon supports, essential for the realization of practical and durable fuel cell systems.

Alkaline direct ethanol fuel cells (ADEFCs) have emerged as a significant fuel cell type, particularly for portable and transportation applications, owing to their high theoretical energy density (8 kWh kg⁻¹), environmental friendliness, and the ease of handling ethanol compared to other fuels like hydrogen.⁹⁸ Ethanol, with advantages such as production from agricultural products, relatively non-toxic fuel, and lower crossover from the anode to the cathode, presents distinct merits over methanol. Despite these benefits, ADEFCs face a critical challenge in the development of cost-effective, highly active, and stable electrocatalysts for the ethanol oxidation reaction (EOR) at the anode.⁹⁹ Addressing the impediment of sluggish kinetics in the EOR, Wolf et al. focused on the synthesis of a PdNiBi nanocatalyst supported on reduced graphene oxide (rGO) through a facile synthesis method.¹⁰⁰ Successful anchoring of PdNiBi nanoparticles onto the rGO support was achieved using the modified instant reduction method. Physicochemical analyses revealed a characteristic two-dimensional wrinkled sheet morphology associated with graphene-based materials. Additionally, the analyses demonstrated uniform and well-distributed metal particles, featuring an average diameter of 2.6 nm on the carbon support. This distribution was attributed to strong C–O–M (M = metal sites) bridges formed by the remaining oxygen functionalities of the rGO. Electrochemical tests highlighted the PdNiBi/rGO composite superior performance for EOR activity and stability compared to commercial Pd/C. The enhanced electrocatalytic activity was attributed to the generation of abundant active sites facilitated by the rGO support and the presence of oxophilic Ni and Bi elements.

2. 8. Graphene and Graphene-Based Materials as Active Components for Electrocatalysis

Among metal-free electrocatalysts the development of electrocatalysts, carbon-based nanomaterials exhibit many advantageous properties, such as variously tunable chemical structures, large surface area, thermal stability, conductivity, excellent mechanical properties, and high durability in various electrochemical environments.^{89–93,101–106} These properties ensure that the materials that serve as catalysts are inexpensive and have high tolerance to a wide pH range. In contrast, pristine carbon nanomaterials exhibit low electrocatalytic activity. Therefore, various approaches have been developed to modify carbon structures and generate electronic structures with highly active catalytic activities. These modifications are achieved by localized distribution of charge and spin density.¹⁰⁷

One strategy for fine-tuning the electronic properties of carbon nanostructures involves introducing intrinsic defects or increasing the edge structure. Among the various defects, the effect of point and line defects in

graphene clusters was investigated using the DFT method on the catalytic ORR activity. The point defects used in the study were Stone-Wales defect, single vacancies, double vacancies, and substituting pentagonal ring and for one dimensional line defects pentagon-heptagon and pentagon-pentagon-octagon chains were used. It was found that the defects can generate spin density and catalyze ORR, similar to the graphene edges.¹⁰⁸

Second possibility is to dope the carbon nanostructure with heteroatoms. The most popular heteroatoms are nitrogen (N), phosphorous (P) and boron (B)^{109–112} or bonds with oxygen (O), sulfur (S), chlorine (Cl), bromine (Br) and iodine (I)^{113,114} atoms at the edges. The different electronegativity of carbon and heteroatoms changes the local charge and spin density, which can have a positive effect on catalytic activity. The active sites in heteroatom-doped carbon nanostructures are the carbon atoms near the dopant, the carbon atoms at the edges, or the dopant itself. For ORR activity, the density functional theory (DFT) calculations showed that heteroatom doping with N, P, B, S, Cl, Br, and I significantly change the charge and spin density and further increases the activity. It was also shown that oxygen functional groups such as –C–OH–, –C=O and –COOH near the edge enhance the ORR activity.¹¹⁵

The third technique is physisorption of organic compounds to the graphene derivative nanostructures. It involves various organic molecules (TCNE, C₃N₄, etc.) adsorbed onto carbon nanotubes or graphene nanostructures. The catalytic potential results from electron transfer either between the organic compound and the graphene derivative. Electron transfer creates electrocatalytically active sites on carbon atoms with higher charge density.^{116,117}

In 2010, nitrogen-doped graphene (N-graphene) has been successfully synthesized through chemical vapor deposition (CVD) of methane in the presence of ammonia.¹¹⁸ This novel N-graphene exhibits remarkable electrocatalytic activity, long-term operational stability, and crossover tolerance superior to platinum when employed as a metal-free electrode for oxygen reduction through the four-electron pathway in alkaline fuel cells. This study marks the pioneering use of graphene and its derivatives as metal-free catalysts for oxygen reduction. The incorporation of nitrogen into the graphene structure plays a pivotal role in enhancing the oxygen reduction reaction (ORR). The N-graphene film outperforms Pt/C electrodes, showcasing a threefold increase in steady-state catalytic current over a broad potential range. Additionally, its long-term stability, crossover tolerance, and resistance to CO poisoning surpass those of Pt/C for oxygen reduction in alkaline electrolytes. This work not only underscores the versatility of N-doping in ORR, as demonstrated with nitrogen-doped carbon nanotubes and N-graphene, but also suggests broader implications for the development of diverse metal-free ORR catalysts for fuel cell applications.

Graphene derivatives doped with nitrogen have emerged as promising non-noble metal materials for the

ORR in both proton exchange membrane and alkaline fuel cells.^{118–120} Nosan et al. developed a rapid and scalable electrical induction heating method for the preparation of nitrogen-doped heat-treated graphene oxide derivatives.¹²¹ Materials synthesized using this method exhibited significantly elevated specific surface areas and demonstrated improved ORR activity compared to conventional synthesis approaches. Interestingly, the authors demonstrated that the temperature program of induction heating could finely modulate the concentration of nitrogen functionalities. Specifically, the amount of graphitic-N configuration increased directly proportional to the final temperature employed, coinciding with enhanced ORR activity in both alkaline and acidic electrolytes, suggesting that the concentration of graphitic-N could be responsible for the increased ORR activity. These findings contribute valuable insights for the development of non-metal nitrogen-doped heat-treated graphene oxide derivatives for applications in energy conversion systems.

The hydrogen evolution reaction (HER) and oxygen evolution reaction (OER) play a pivotal role in the field of electrocatalysis, particularly in the context of water electrolyzers, where they serve as the cathodic and anodic half-reactions, respectively.^{122–126} HER involves the reduction of protons to produce molecular hydrogen and OER involves the conversion of water into oxygen and protons, crucial processes for the sustainable generation of hydrogen gas as a clean and renewable energy carrier. Efficient electrocatalysis of the HER and OER are imperative for enhancing the overall performance and economic viability of water electrolyzers, as it determines the rate at which hydrogen and oxygen are produced and influences the system's energy efficiency.^{127–131} Electrodes with high catalytic activity for HER and OER facilitate lower overpotentials, reducing the energy input required for hydrogen and oxygen evolution.^{132–136} Consequently, advancements in the design and development of electrocatalysts for HER and OER have significant implications for the scalability and commercialization of water electrolysis technologies, offering a pathway towards the realization of a clean and sustainable hydrogen economy.

Zheng et al. study presents the synthesis of a metal-free electrocatalyst, comprising exclusively carbon and nitrogen components, achieved through the integration of graphitic carbon nitride (g-C₃N₄) and nitrogen-doped graphene (N-graphene; NG).¹³⁷ The resulting C₃N₄@NG hybrid exhibits distinctive molecular architecture and electronic characteristics, rendering it suitable for electrocatalytic hydrogen evolution reaction (HER) applications. Despite not reaching the activity levels of state-of-the-art Pt catalysts, this metal-free hybrid demonstrates HER performance comparable to well-established metallic counterparts, including nanostructured MoS₂ materials. Experimental observations, complemented by density functional theory (DFT) calculations unveil the unique electrocatalytic properties arising from a synergistic effect within this

hybrid nanostructure: g-C₃N₄ furnishes highly active hydrogen adsorption sites, while N-graphene facilitates the electron-transfer process during proton reduction. These results demonstrate the potential of well-designed metal-free catalysts, comparable to precious metals, for highly efficient electrocatalytic HER. Consequently, this work opens a promising avenue for the broader utilization of metal-free alternative materials, reducing reliance on noble metals across diverse applications.

Jiao et al. systematically explored the HER across a range of non-metal heteroatom-doped graphene materials, incorporating nitrogen, phosphorus, oxygen, sulfur, and boron.¹³⁸ Employing electrochemical reaction rate measurements and density functional theory (DFT) calculations to assess adsorption energetics, the study established a correlation between current density on each material and hydrogen adsorption strength on molecular models. The integrated experimental and theoretical analysis revealed that the suboptimal catalytic activity of carbon-based catalysts stems from weak hydrogen adsorption on graphene surfaces. A distinctive volcano-shaped relationship emerged, linking the activity (current density) to the free energy of hydrogen adsorption, with an optimal doped-graphene electrocatalyst predicted to reside at the volcano's apex. To validate this hypothesis, the researchers fabricated and evaluated three co-doped graphene samples (nitrogen-sulfur, nitrogen-phosphorus, and nitrogen-boron), calculating their hydrogen adsorption energy using DFT. Both experimental and theoretical results converged, demonstrating that nitrogen-sulfur co-doped graphene emerged as the most active catalyst, attributed to its lowest hydrogen adsorption energy. This enhancement in activity is postulated to arise from a synergistic coupling effect between the two heteroatoms, highlighting the potential for tailored multi-element doping or the introduction of structural defects to engineer idealized doped graphene electrocatalysts for improved HER performance.

Zhao et al. study presents an investigation into the electrocatalytic activity of nitrogen-doped graphite nano-materials derived from a nitrogen-rich polymer.¹³⁹ These materials exhibit superior performance in the oxygen evolution reaction (OER) in alkaline environments compared to conventional electrocatalysts. Remarkably, in the absence of transition metals, the optimized nitrogen/carbon materials demonstrate OER overpotentials as low as 0.38 V at a current density of 10 mA cm⁻² at pH 13, surpassing other non-metal OER electrocatalysts. Comprehensive electrochemical and physical analyses reveal that the improved OER activity of the nitrogen/carbon materials arises from active sites associated with pyridinic-N and/or quaternary-N functionalities. Specifically, carbon atoms adjacent to nitrogen atoms are postulated to be positively charged due to the electron-withdrawing nature of nitrogen atoms in a graphene π -system. This positive charge facilitates the absorption of OH⁻ ions by the positively charged carbon, a phenomenon crucial for OER. In the

context of the limiting step of OER, the authors consider one plausible explanation is that the neighboring positive-charged carbon atoms aid the facile recombination of two oxygen adsorbed species (O_{ads}). Finally, the authors suggest that another potential mechanism may involve nitrogen atoms, as their density of state in a graphitic sp^2 carbon network is proximate to the Fermi level.^{140,141} Noteworthy, further studies corroborated with these findings.^{142,143}

Hydrogen peroxide (H_2O_2) serves as an environmentally friendly oxidizing agent with diverse applications, prompting the exploration of alternative, efficient routes for its production. The two-electron oxygen reduction reaction ($2e^-$ ORR) emerges as a promising avenue, offering an attractive alternative to the energy-intensive anthraquinone oxidation process. However, conventional catalysts for $2e^-$ ORR fall short of meeting industrial demands. Addressing this, Lee et al. synthesized 3D graphene catalysts with controlled oxygen functional groups and defects, achieved through a one-step aerosol spray drying process.¹⁴⁴ A systematic investigation into the structure-electrochemical performance relationship of these graphene catalysts underscored the decisive role of oxygen functional groups and defects in facilitating H_2O_2 production. The optimized graphene catalyst demonstrated exceptional H_2O_2 selectivity (92–100%) across a wide potential range with remarkable stability and a high production rate at 0.4 V vs. RHE (ca. 450 mmol $g_{cat}^{-1} h^{-1}$). Complementary DFT calculations elucidated the contribution of diverse oxygen functional groups and defect sites to the $2e^-$ ORR pathway, establishing a scaling relation between OOH and O adsorption strengths. This thorough investigation establishes a critical structure-mechanism-performance relationship for nanostructured carbon systems in $2e^-$ ORR, offering crucial insights for the design of highly active and selective metal-free carbon electrocatalysts for H_2O_2 production, achievable through the precise tuning of oxygen functional groups and defect structures.

3. Flash Joule Heating (FJH) Method for Bulk Graphene Production

Flash Joule heating (FJH) is an electro-resistive method used for the synthesis of a broad spectrum of materials. As its name suggests, the method relies on the joule heat produced by the passage of rapid pulses of high-density electrical current through a conductive material. Unlike most other thermal methods where heat (or energy flux which gets converted to heat) from an external source is applied on the surface and then penetrates through the material in a process limited by the thermal conductivity of the sample, in FJH the heat is distributed uniformly throughout the whole volume. This feature allows very rapid heating rates in short periods of time, i.e. “in a flash”.

Joule heating has been in use for the sintering of materials for a long time and under different modifications lies in the basis of numerous processes. Under the umbrella term “resistance sintering”, Orrù et al. summarized 60 different process names by their first appearance in literature.¹⁴⁵ In another review article, Grasso et al. trace the history of the technology back to the patent submitted by Bloxam from 1906 as “the first patent on pure direct current (DC) resistance sintering”.¹⁴⁶ Despite the various processing parameters that differentiate the existing techniques, they are all based on the same physical phenomenon, the usage of the Joule heat for the synthesis of materials.

Since the early 20th century, the FJH technology has been applied to a wide variety of advanced materials, but only recently it was used for the synthesis of graphene by Luong and co-authors.⁸ The graphene and its derivatives synthesized using FJH deserve significant attention, because of the remarkable properties reported. These properties are attributed to the rotationally disordered or turbostratic structure of the flash graphene.¹⁴⁷ The turbostratic arrangement of the individual graphene layers (or rotational mismatching about the axis normal to the graphene sheets) is a direct result of the rapid cooling rate. Specifically, the extremely fast temperature change (on the order of $10^4 K s^{-1}$) during the cooling process impedes the produced flash graphene (FG) to not assume the thermodynamically favored arrangement and stacking of the graphene sheets (Bernal AB-stacked form).¹⁴⁸

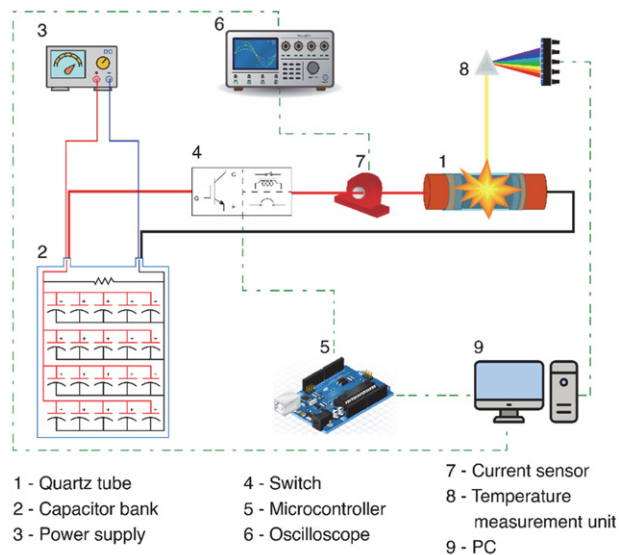


Figure 2. Typical flash Joule heating (FJH) setup diagram.

The Flash Joule Heating (FJH) process is typically conducted in a quartz tube (Figure 2 – element 1), chosen for its high thermal resistance. In this setup, a small quantity of carbonaceous material is placed between two graphite electrodes, which apply compression from both sides

until the desired electrical resistance is achieved. Since the FJH process requires rapid, high-current pulses that standard power grids cannot supply in such a brief time span, a large capacitor bank (Figure 2 – element 2) is generally used. This capacitor bank is charged to hundreds of volts, temporarily storing the necessary electrical energy, which is then swiftly discharged into the sample. A specialized electrical switch (Figure 2 – element 4), capable of handling the high current, is employed to control this discharge. As the flash process occurs within milliseconds, the switch is typically controlled by a microcontroller (Figure 2 – element 5) that manages the rapid release of the capacitor's energy into the sample and halts the process once the pre-set pulse duration is reached. During the process, an oscilloscope (Figure 2 – element 6) monitors the current and voltage in the system for detailed analysis. Temperature measurement is performed using an optical device (Figure 2 – element 8) that detects the light emitted by the heated carbon material, which is then compared to the spectrum of a grey body to estimate the temperature. When the pulse duration is completed, the electrical switch disconnects the circuit, ceasing the discharge and stopping further heat generation. From this point, the sample cools rapidly by natural means, typically 10^4 K s^{-1} . The temperatures reached in this process can exceed 3,000 K. At this temperature, all chemical bonds get broken and almost all the hetero atoms that are more volatile than carbon (O, H, N, S, P, etc.) leave the system through outgassing. This allows the use of a wide range of materials as precursors to produce turbostratic FG. Almost any carbon-based precursor can be transformed into bulk quantities of graphene.¹⁴⁹ Since no toxic and/or corrosive chemicals, solvents, and reactive gases are used, FJH offers a cheap and environmentally friendly method for the recycling of waste materials. Particularly, one of its key advantages over the traditional technologies for the synthesis of graphene is the possibility of upcycling low-value materials into high-value nanomaterials. Carbon-containing wastes and byproducts of different origins that often have little to no practical value require disposal or expensive utilization and even pose environmental hazards can be used as feedstock for flash graphene. For example, Luong and co-authors have shown the use of coal, coke, and even negative value materials such as waste plastics, rubber tires and discarded food can be processed into FG with purity greater than 99%.⁸

In terms of applicability, Tour and co-authors report that the FG produced shows higher quality compared to bulk graphene flakes produced using traditional methods (e.g., LPE and Oxidation with successive reduction). For instance, their carbon black-derived FG was used to prepare cement composites which showed compressive and tensile strength three times larger than those of other reported graphene-cement composites with the same loading.⁸ In another work, FG prepared from rubber waste was again used as a reinforcing additive to cement and led to a

~30% increase in concrete strength.¹⁵⁰ Hence, if the FG production can be implemented on industrial scale, it would have a significant impact on our world. Stronger cement would lead to a reduction in the amount of concrete needed, which in turn can result in significant carbon emission reduction as the cement industry is one of the main sources of greenhouse gases, accountable for 5–7% of the global anthropogenic carbon dioxide emissions,¹⁵¹ and at the same time represents ca. 7% of the industrial energy consumption.¹⁵²

When FG (in this case derived from metallurgical coke)¹⁵³ is applied as an additive in epoxy composites, the resulting composites have shown record high loading ratios that haven't been reported in the literature. Although graphene and other carbon nanomaterials have shown to improve the mechanical properties of epoxies, their high production costs limit their use on an industrial scale.¹⁵³ Since FG can be produced inexpensively and from low value material sources, it has been successfully used as a reinforcing and filler agent at weight ratios up to 50%. The resulting composites show a significant increase in Young's modulus, hardness, compressive strength and maximum elongation, as well as an impressive 496% increase in toughness compared to FG-free composites. Furthermore, the addition of such high amounts of FG to the epoxy composites resulted in a reduction of greenhouse gas emissions, and water and energy consumption during production by more than a third compared to the pure epoxy, making FG a promising candidate for a more sustainable chemical industry.¹⁵³ In terms of sustainability FJH offers additional advantages. Since the electrical energy used for the process is temporarily stored in a capacitor bank, FJH can act as a flexible load, meaning it can adjust its power consumption based on the availability of renewable electricity. Induction heating as well as other high temperature methods can benefit from the same source, but cannot compete with the ease, efficiency and speed offered by FJH.¹²¹ Moreover, it was demonstrated that the application of electric current through the sample can facilitate the crystallization of graphene, leading to the formation of a higher quality product.¹⁵⁴

4. Flash Graphene (FG) Applied to Electrocatalysis

The need to address rising energy consumption and environmental concerns requires the development of sustainable and environmentally friendly energy storage and conversion technologies. Promising innovations in the field of energy conversion include fuel cells and electrolyzers integrated into the electrochemical water cycle. This cycle revolves around oxygen reduction (ORR), oxygen evolution (OER), hydrogen evolution (HER), and hydrogen oxidation (HOR), central processes for the production of electricity, hydrogen, or chemical compounds. The effectiveness and accessibility of these energy solutions de-

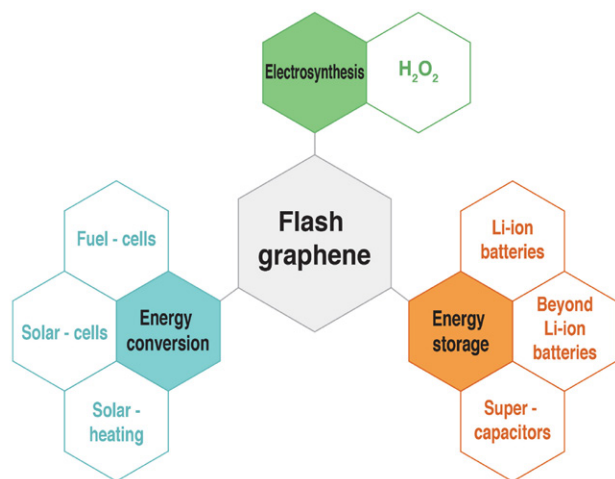


Figure 3. Diverse applications of flash graphene and other carbon allotropes.

pend largely on the catalysts used. The most effective catalysts are currently based on precious metals such as platinum, but their scarcity and exorbitant costs prevent their widespread use. Therefore, there is an urgent need for innovations in catalysts that not only offer better performance and longevity but are also economically viable and do not require precious metals.^{107,155}

Because the application of high-quality graphene and its derivatives for energy storage and conversion necessarily requires large quantities to be produced at industrial scale, FJH promises to have a tremendous influence in this field in the years to come (Figure 3). Although the use of FJH to produce FG and its derivatives is a relatively new technology, a few noteworthy examples for the application of FG in electrocatalysis already exist. Wyss and co-authors used the FJH process to produce holey and wrinkled flash graphene (HWFG) from mixed plastic waste. Among the applications demonstrated, HWFG was used as electrocatalyst for the hydrogen evolution reaction (HER) in acidic media in view of its high concentration of pores and edge defects.¹⁵⁶ When derived from high-density polyethylene (HDPE), HWFG electrocatalyst showed an overpotential of 613 mV (versus reversible hydrogen electrode, RHE) for hydrogen evolution in acidic media (Figure 4). Moreover, due to HWFG high surface area and porous structure, hydrogen gas (H_2) can easily escape as it evolves from HWFG active sites, allowing for constant H_2 production over time. Because FJH synthesis process does not involve the use of transition metals, the HWFG activity for HER is solely related to carbon-based surface-active sites. Consequently, HWFG showed very promising stability for 20 hours test, and even a slightly overpotential decrease (19 mV) over a -20 mA cm^{-2} current density, which was ascribed to the creation of more defects by cavitation caused by the H_2 constant evolution.

Graphene doping is a well-known strategy to create electrocatalytic active sites within graphene sheets.¹⁰² Because of the harsh reagents usually employed for top-down

synthesis of heteroatom-doped graphene (e.g., graphene oxide doping¹⁵⁷), the possibility of producing heteroatom-doped FG with high quality and impurity-free graphene flakes in bulk quantities at low-cost may open opportunities for its broad implementation in energy storage and conversion applications. In a recent work, Chen and co-authors used the FJH method to synthesize graphene doped by different heteroatoms in bulk quanti-

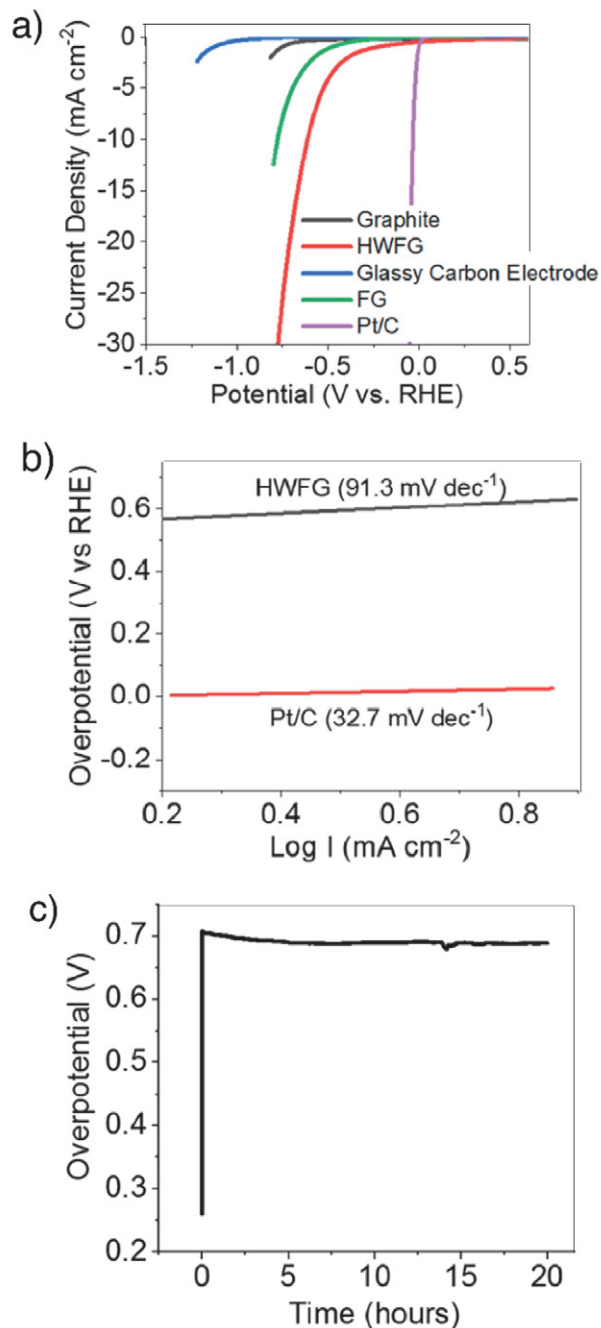


Figure 4. Assessment of HER electrochemical activity of mixed PW HWFG: a) Linear scan voltammograms; b) Tafel slope; c) Stability testing of HWFG at -20 mA/cm^2 . Graphs reproduced from reference.¹⁵⁶ HWFG = holey and wrinkled flash graphene. FG = flash graphene. Pt/C = platinum nanoparticles supported on carbon.

ties.¹¹¹ Both doped (boron, nitrogen, oxygen, phosphorous, and sulfur) and co-doped (when more than one element is used) FG showed high quality, similar to undoped FG, i.e. turbostratic structure, larger interlayer spacing between graphene sheets, and remarkable dispersibility. When applied as electrocatalysts for the oxygen reduction reaction (ORR) in alkaline media (Figure 5), sulfur-doped FG showed the highest activity, with a potential of 0.88 V (versus RHE) at a current density of -0.2 mA cm^{-2} , and a Tafel slope of 74 mV dec^{-1} . This result is in line with previous theoretical studies, where density functional theory (DFT) calculations revealed that sulfur-doped graphene

clusters can be a competitive electrocatalyst for ORR depending on their doping structures.¹¹⁴

A widely adopted strategy for enhancing and selectively tuning the electrocatalytic properties of graphene is the introduction of defects into its crystal structure. In a paper published by S. Dong and co-workers flash joule heating is used as a new approach for reducing graphene oxide using an exceptionally brief flash duration of a mere 1 ms. This approach enables the fabrication of defective graphene without intricate functional groups. The resulting material harbors a multitude of defects, and its unique three-dimensional structure allows it to withstand high

a) Flash Joule heating and doping

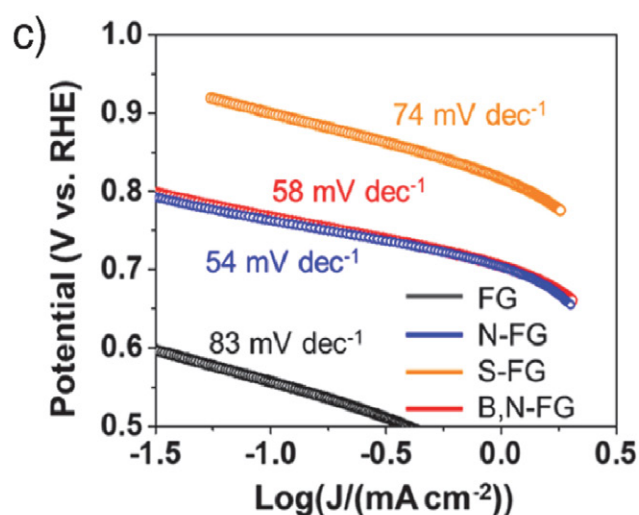
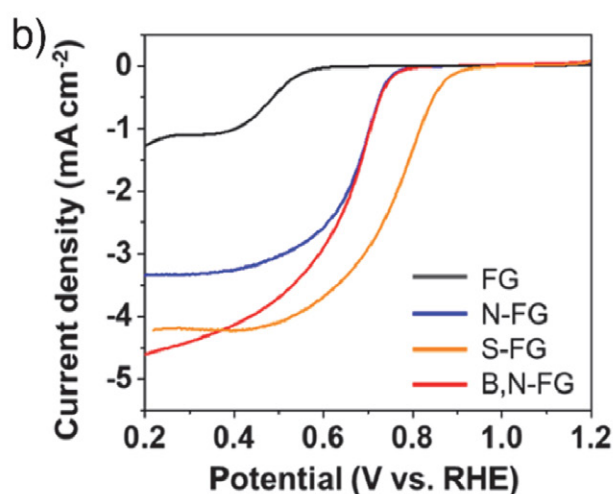
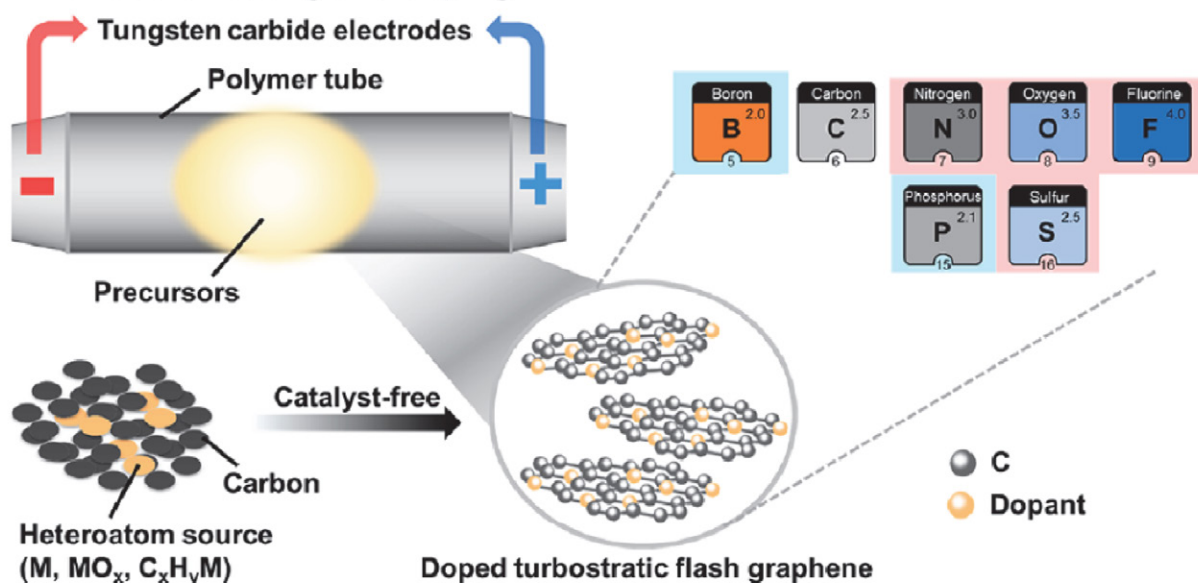


Figure 5. Electrochemical characterization of electrocatalysts synthesized by Flash Joule heating (FJH): a) Schematic representation of heteroatom-doped turbostratic graphene synthesis via FJH; b) Comparison of the oxygen reduction reaction performance among variously doped functionalized flash graphene in 0.1 M KOH solution at 1600 rpm; c) Corresponding Tafel plots. Image and graphs reproduced from reference.¹¹¹ FG = flash graphene. N-FG = nitrogen-doped flash graphene. S-FG = sulfur-doped flash graphene. B,N-FG = boron-nitrogen-doped flash graphene.

currents and prolonged cycles without drastic failures when used as an anode material in LIBs. It exhibits a remarkable reversible capacity of 1007 mAh/g after 5000 cycles at the current density of 5 A/g – surpassing the performance of graphene modified by other techniques.¹⁵⁸

Several studies have highlighted the feasibility of flash joule heating as an effective method for recycling and regenerating graphite from spent lithium-ion batteries. Natural graphite is classified as a critical raw material by the European Union, highlighting its strategic importance. To achieve true sustainability, it is essential to develop robust recycling programs for graphite, which are currently not widely established. In another study, S. Dong and co-workers utilized flash joule heating to recycle graphite from end-of-life lithium-ion batteries, demonstrating that the recycled graphite outperforms new commercial graphite in terms of electrical conductivity. Their comparison with other recent methods shows that the anodic graphite recovered through FJH exhibits higher initial Coulombic efficiency, near-complete capacity recovery, and is produced at significantly lower cost, all while requiring minimal processing time thus showing great potential for commercial applications.¹⁵⁹ In a more recent study, Tour et. al demonstrated an ultrafast flash recycling method to regenerate the graphite anode. During this process the intrinsic 3D layered graphite core structure is preserved and is coated with a solid-electrolyte-interphase derived carbon shell, contributing to high initial specific capacity, superior rate performance, and cycling stability, when compared to anode materials recycled using a high-temperature-calcination method. An additional advantage of the process is that it allows the extraction of metal ions from the flashed anode waste with average recovery efficiency reaching >99% using just 0.1M HCl.¹⁶⁰

Since this technology is in its initial state of development and application, the literature lacks comprehensive studies directly comparing the electrocatalytic properties of flash-graphene (FG) to those of the well-established carbon materials, the results available thus far affirm that flash joule heating is an exceptionally robust and sustainable method for synthesizing carbon-based electrocatalysts.

5. Perspective and Closing Remarks

In the fields of materials science and clean energy technologies, flash Joule heating (FJH) stands out as a groundbreaking method poised to revolutionize the large-scale production of graphene and simultaneously open new pathways for advanced recycling, upcycling and utilization of waste materials. This innovative technique harnesses the renewable power of high electric currents to rapidly elevate carbon-containing precursors to extreme temperatures, leading to the formation of turbostratic graphene (flash graphene (FG)). The remarkable attributes of FJH offer a new perspective on graphene manufacturing, effectively addressing longstanding challenges in the

industry. One of the most compelling aspects of FJH is its exceptional speed, with heating times measured in milliseconds. This rapid processing capability not only enables high production throughput but also promises to alleviate one of the critical bottlenecks in graphene manufacturing. Furthermore, FJH exhibits a unique ability to utilize a wide range of carbon sources, including biomass and waste materials, aligning with the pursuit of sustainability and economic viability in materials production. This versatility, combined with the method's minimal waste generation, results in flash graphene with exceptional crystallinity, endowing it with superior electrical and thermal conductivity. These attributes are of paramount importance for various energy-related applications. As we consider the implications of FJH on a broader scale, it becomes evident that its scalability, versatility, and efficiency position it as a game-changer in graphene production. This transformative approach offers a promising pathway toward unlocking the full commercial potential of graphene across various industries, particularly in energy storage and conversion. In the context of clean energy, the imperative for innovation extends beyond materials production to catalysis. Electrochemical processes such as oxygen reduction reaction (ORR), oxygen evolution reaction (OER), hydrogen evolution reaction (HER), and hydrogen oxidation reaction (HOR) are pivotal in energy conversion and storage devices like fuel cells, electrolyzers, and metal-air batteries. Catalysts play a crucial role in accelerating these reactions, but their efficiency and cost-effectiveness are of utmost importance. Traditional precious metal catalysts, notably platinum, face limitations due to their scarcity and high cost, driving the need for alternative, metal-free catalysts. Herein lies the significance of carbon-based nanomaterials as electrocatalysts, particularly in the context of graphene. These materials offer a plethora of advantages, high thermodynamic stability including tunable structures, high surface area, thermal stability, and conductivity. However, pristine carbon nanomaterials exhibit limited electrocatalytic activity. Innovative strategies such as introducing intrinsic defects or edge structures, doping with heteroatoms, and physisorption of organic compounds have emerged to enhance their catalytic performance. The manipulation of carbon nanostructures through these techniques has yielded promising results. Point and line defects, as well as heteroatom doping, can generate charge and spin density, catalyzing crucial electrochemical reactions. Moreover, the physisorption of organic compounds onto graphene derivatives fosters electron transfer and creates electrocatalytically active sites, contributing to improved performance. In the quest for large-scale production of high-quality graphene and its derivatives for energy applications, FJH holds great promise. Recent examples of its application in electrocatalysis, such as holey and wrinkled flash graphene (HWFG) for the hydrogen evolution reaction (HER), showcase its potential in energy conversion. Notably, FJH-derived materials exhibit impressive

stability and cost-effective performance, devoid of transition metals, reaffirming the pivotal role of carbon-based surface-active sites in electrocatalysis.

As this novel method was only developed relatively recently in 2020,⁸ there are still some challenges and obstacles to overcome for wider applicability. Many of the key challenges for scaling flash graphene production identified in the literature are related to the need for a deeper understanding and precise control of the processes occurring during FJH, which can vary depending on the specific feedstock used. In addition, life cycle assessments (LCA) of the production process and its overall environmental impact are essential. This requires the development of advanced computer models and process optimization as well as the implementation of comprehensive quality control protocols and standardization of the resulting graphene products.^{161,162} The reported ongoing industrial scaled up to 1 ton per day by early 2023 and targeted for 100 tons per day by 2024,¹⁶³ at an electricity cost of around \$100 per ton of graphene produced emphasize the promising future of the technology.

As we look ahead, the convergence of FJH and graphene-based electrocatalysis represents a paradigm shift in clean energy solutions. The integration of scalable and sustainable materials production with advanced catalytic systems holds the key to unlocking the full potential of renewable energy technologies. The journey of scientific exploration and development in these domains promises a brighter and more sustainable future, where the marriage of innovation and sustainability will lead us towards cleaner, more efficient energy solutions.

Acknowledgment

The authors would like to thank the Slovenian Research and Innovation Agency (ARIS) for funding through Research programme: P2-0423 and Research project J7-4636.

6. References

1. K. S. Novoselov, A. K. Geim, S. V. Morozov, D. Jiang, Y. Zhang, S. V. Dubonos, I. V. Grigorieva, A. A. Firsov, *Science* **2004**, *306*, 666–669. DOI:10.1126/science.1102896
2. K. S. Novoselov, *Rev. Mod. Phys.* **2011**, *83*, 837–849. DOI:10.1103/RevModPhys.83.837
3. A. K. Geim, *Rev. Mod. Phys.* **2011**, *83*, 851–862. DOI:10.1103/RevModPhys.83.851
4. T. A. Land, T. Michely, R. J. Behm, J. C. Hemminger, G. Comsa, *Surf. Sci.* **1992**, *264*, 261–270. DOI:10.1016/0039-6028(92)90183-7
5. M. Orlita, C. Faugeras, P. Plochocka, P. Neugebauer, G. Martinez, D. K. Maude, A.-L. Barra, M. Sprinkle, C. Berger, W. A. de Heer, M. Potemski, *Phys. Rev. Lett.* **2008**, *101*, 267601. DOI:10.1103/PhysRevLett.101.267601
6. C. Lee, X. Wei, J. W. Kysar, J. Hone, *Science* **2008**, *321*, 385–388. DOI:10.1126/science.1157996
7. A. C. Ferrari, F. Bonaccorso, V. Fal'ko, K. S. Novoselov, S. Roche, P. Bøggild, S. Borini, F. H. L. Koppens, V. Palermo, N. Pugno, J. A. Garrido, R. Sordan, A. Bianco, L. Ballerini, M. Prato, E. Lidorikis, J. Kivioja, C. Marinelli, T. Ryhänen, A. Morpurgo, J. N. Coleman, V. Nicolosi, L. Colombo, A. Fert, M. Garcia-Hernandez, A. Bachtold, G. F. Schneider, F. Guinea, C. Dekker, M. Barbone, Z. Sun, C. Galiotis, A. N. Grigorenko, G. Konstantatos, A. Kis, M. Katsnelson, L. Vandersypen, A. Loiseau, V. Morandi, D. Neumaier, E. Treossi, V. Pellegrini, M. Polini, A. Tredicucci, G. M. Williams, B. Hee Hong, J.-H. Ahn, J. Min Kim, H. Zirath, B. J. van Wees, H. van der Zant, L. Occhipinti, A. Di Matteo, I. A. Kinloch, T. Seyller, E. Quesnel, X. Feng, K. Teo, N. Rupesinghe, P. Hakonen, S. R. T. Neil, Q. Tannock, T. Löfwander, J. Kinaret, *Nanoscale* **2015**, *7*, 4598–4810. DOI:10.1039/C4NR01600A
8. D. X. Luong, K. V. Bets, W. A. Algozeeb, M. G. Stanford, C. Kittrell, W. Chen, R. V. Salvatierra, M. Ren, E. A. McHugh, P. A. Advincula, Z. Wang, M. Bhatt, H. Guo, V. Mancevski, R. Shahsavari, B. I. Yakobson, J. M. Tour, *Nature* **2020**, *577*, 647–651. DOI:10.1038/s41586-020-1938-0
9. A. K. Geim, K. S. Novoselov, *Nat. Mater.* **2007**, *6*, 183–191. DOI:10.1038/nmat1849
10. J. Hou, Y. Shao, M. W. Ellis, R. B. Moore, B. Yi, *Phys. Chem. Chem. Phys.* **2011**, *34*, 15384–15402. DOI:10.1039/c1cp21915d
11. R. Raccichini, A. Varzi, S. Passerini, B. Scrosati, *Nat. Mater.* **2015**, *14*, 271–279. DOI:10.1038/nmat4170
12. M. F. El-Kady, Y. Shao, R. B. Kaner, *Nat. Rev. Mater.*, **2016**, *7*, 1–14. DOI:10.1038/natrevmats.2016.33
13. X. Chen, R. Paul, L. Dai, *Natl. Sci. Rev.* **2017**, *4*, 453–489. DOI:10.1093/nsr/nwx009
14. K. S. Novoselov, V. I. Fal'ko, L. Colombo, P. R. Gellert, M. G. Schwab, K. Kim, *Nature* **2012**, *490*, 192–200. DOI:10.1038/nature11458
15. A. Bianco, H.-M. Cheng, T. Enoki, Y. Gogotsi, R. H. Hurt, N. Koratkar, T. Kyotani, M. Monthieux, C. R. Park, J. M. D. Tascon, J. Zhang, *Carbon N Y* **2013**, *65*, 1–6. DOI:10.1016/j.carbon.2013.08.038
16. L. Lin, H. Peng, Z. Liu, *Nat. Mater.* **2019**, *18*, 520–524. DOI:10.1038/s41563-019-0341-4
17. S. H. Choi, S. J. Yun, Y. S. Won, C. S. Oh, S. M. Kim, K. K. Kim, Y. H. Lee, *Nat. Commun.* **2022**, *13*, 1484. DOI:10.1038/s41467-022-29182-y
18. S. Park, *Nat. Rev. Mater.* **2016**, *1*, 1–2. DOI:10.1038/natrevmats.2016.80
19. W. Kong, H. Kum, S. H. Bae, J. Shim, H. Kim, L. Kong, Y. Meng, K. Wang, C. Kim, J. Kim, *Nat. Nanotechnol.* **2019**, *14*, 927–938. DOI:10.1038/s41565-019-0555-2
20. Editorial, *Nat. Mater.* **2019**, *18*, 519. DOI:10.1038/s41563-019-0394-4
21. P. Bøggild, *Nat. Commun.* **2023**, *14*, 1126. DOI:10.1038/s41467-023-36891-5
22. A. Zurutuza, C. Marinelli, *Nat. Nanotechnol.* **2014**, *9*, 730–734. DOI:10.1038/nnano.2014.225

23. W. Ren, H.-M. Cheng, *Nat. Nanotechnol.* **2014**, *9*, 726–730. DOI:10.1038/nnano.2014.229
24. C. A. Clifford, E. H. Martins Ferreira, T. Fujimoto, J. Herrmann, A. R. Hight Walker, D. Koltsov, C. Punckt, L. Ren, G. J. Smallwood, A. J. Pollard, *Nat. Rev. Phys.* **2021**, *3*, 233–235. DOI:10.1038/s42254-021-00278-6
25. S. Milana, *Nat. Phys.* **2021**, *17*, 1068–1068. DOI:10.1038/s41567-021-01339-4
26. A. P. Kauling, A. T. Seefeldt, D. P. Pisoni, R. C. Pradeep, R. Bentini, R. V. B. Oliveira, K. S. Novoselov, A. H. Castro Neto. *Adv. Mater.* **2018**, *30*, 1803784. DOI:10.1002/adma.201803784
27. P. Bøggild, *Nature* **2018**, *562*, 502–503. DOI:10.1038/d41586-018-06939-4
28. T. Barkan, *Nat. Nanotechnol.* **2019**, *14*, 904–906. DOI:10.1038/s41565-019-0556-1
29. X.-Y. Wang, A. Narita, K. Müllen, *Nat. Rev. Chem.* **2017**, *2*, 0100. DOI:10.1038/s41570-017-0100
30. M. Batzill, *Surf. Sci. Rep.* **2012**, *67*, 83–115. DOI:10.1016/j.surfrep.2011.12.001
31. A. L. Higginbotham, D. V Kosynkin, A. Sinitskii, Z. Sun, J. M. Tour, *ACS Nano* **2010**, *4*, 2059–2069. DOI:10.1021/nn100118m
32. L. Jiao, X. Wang, G. Diankov, H. Wang, H. Dai, *Nat. Nanotechnol.* **2010**, *5*, 321–325. DOI:10.1038/nnano.2010.54
33. C. Zhang, Z. Peng, J. Lin, Y. Zhu, G. Ruan, C.-C. Hwang, W. Lu, R. H. Hauge, J. M. Tour, *ACS Nano* **2013**, *7*, 5151–5159. DOI:10.1021/nn400750n
34. J. Lim, U. Narayan Maiti, N.-Y. Kim, R. Narayan, W. Jun Lee, D. Sung Choi, Y. Oh, J. Min Lee, G. Yong Lee, S. Hun Kang, H. Kim, Y.-H. Kim, S. Ouk Kim, *Nat. Commun.* **2016**, *7*, 10364. DOI:10.1038/ncomms10364
35. H. Wang, Y. Wang, Z. Hu, X. Wang, *ACS Appl. Mater. Interfaces* **2012**, *4*, 6827–6834. DOI:10.1021/am302000z
36. B. Xiao, X. Li, X. Li, B. Wang, C. Langford, R. Li, X. Sun, *J. Phys. Chem. C* **2014**, *118*, 881–890. DOI:10.1021/jp410812v
37. Y. Song, H. Hu, M. Feng, H. Zhan, *ACS Appl Mater Interfaces* **2015**, *7*, 25793–25803. DOI:10.1021/acsami.5b07700
38. A. Sinitskii, A. Dimiev, D. V Kosynkin, J. M. Tour, *ACS Nano* **2010**, *4*, 5405–5413. DOI:10.1021/nn101019h
39. Q. Shu, Z. Xia, W. Wei, X. Xu, R. Sun, R. Deng, Q. Yang, H. Zhao, S. Wang, G. Sun, *ACS Appl. Energy Mater.* **2019**, *2*, 5446–5455. DOI:10.1021/acsaem.9b00506
40. D. B. Shinde, J. Degupta, A. Kushwaha, M. Aslam, V. K. Pillai, *J. Am. Chem. Soc.* **2011**, *133*, 4168–4171. DOI:10.1021/ja1101739
41. D. V. Kosynkin, A. L. Higginbotham, A. Sinitskii, J. R. Lomeda, A. Dimiev, B. K. Price, J. M. Tour, *Nature* **2009**, *458*, 872–876. DOI:10.1038/nature07872
42. L. Sun, G. Yuan, L. Gao, J. Yang, M. Chhowalla, M. H. Ghahrahcheshmeh, K. K. Gleason, Y. S. Choi, B. H. Hong, Z. Liu, *Nat. Rev. Methods Primers* **2021**, *1*, 5. DOI:10.1038/s43586-020-00005-y
43. C. Mattevi, H. Kim, M. Chhowalla, *J. Mater. Chem.* **2011**, *21*, 3324–3334. DOI:10.1039/C0JM02126A
44. S. Marchini, S. Günther, J. Wintterlin, *Phys. Rev. B* **2007**, *76*, 075429. DOI:10.1103/PhysRevB.76.075429
45. P. Sutter, J. T. Sadowski, E. Sutter, *Phys. Rev. B* **2009**, *80*, 245411. DOI:10.1103/PhysRevB.80.245411
46. J. Lahiri, T. Miller, L. Adamska, I. I. Oleynik, M. Batzill, *Nano Lett* **2011**, *11*, 518–522. DOI:10.1021/nl103383b
47. L. Gao, J. R. Guest, N. P. Guisinger, *Nano Lett.* **2010**, *10*, 3512–3516. DOI:10.1021/nl1016706
48. C.-M. Seah, S.-P. Chai, A. R. Mohamed, *Carbon N Y* **2014**, *70*, 1–21. DOI:10.1016/j.carbon.2013.12.073
49. S. Bhaviripudi, X. Jia, M. S. Dresselhaus, J. Kong, *Nano Lett* **2010**, *10*, 4128–4133. DOI:10.1021/nl102355e
50. X. Li, C. W. Magnuson, A. Venugopal, R. M. Tromp, J. B. Hannon, E. M. Vogel, L. Colombo, R. S. Ruoff, *J. Am. Chem. Soc.* **2011**, *133*, 2816–2819. DOI:10.1021/ja109793s
51. M. Losurdo, M. M. Giangregorio, P. Capezzuto, G. Bruno, *Phys. Chem. Chem. Phys.* **2011**, *13*, 20836. DOI:10.1039/c1cp22347j
52. H. I. Rasool, E. B. Song, M. Mecklenburg, B. C. Regan, K. L. Wang, B. H. Weiller, J. K. Gimzewski, *J. Am. Chem. Soc.* **2011**, *133*, 12536–12543. DOI:10.1021/ja200245p
53. A. Dahal, M. Batzill, *Nanoscale* **2014**, *6*, 2548. DOI:10.1039/c3nr05279f
54. J. Wintterlin, M.-L. Bocquet, *Surf. Sci.* **2009**, *603*, 1841–1852. DOI:10.1016/j.susc.2008.08.037
55. Y. Zhang, L. Gomez, F. N. Ishikawa, A. Madaria, K. Ryu, C. Wang, A. Badmaev, C. Zhou, *J. Phys. Chem. Lett.* **2010**, *1*, 3101–3107. DOI:10.1021/jz1011466
56. Q. Yu, L. A. Jauregui, W. Wu, R. Colby, J. Tian, Z. Su, H. Cao, Z. Liu, D. Pandey, D. Wei, T. F. Chung, P. Peng, N. P. Guisinger, E. A. Stach, J. Bao, S.-S. Pei, Y. P. Chen, *Nat. Mater.* **2011**, *10*, 443–449. DOI:10.1038/nmat3010
57. Y. Zhang, L. Zhang, C. Zhou, *Acc. Chem. Res.* **2013**, *46*, 2329–2339. DOI:10.1021/ar300203n
58. L. P. Biró, P. Lambin, *New J. Phys.* **2013**, *15*, 035024. DOI:10.1088/1367-2630/15/3/035024
59. Y.-M. Lin, C. Dimitrakopoulos, K. A. Jenkins, D. B. Farmer, H.-Y. Chiu, A. Grill, Ph. Avouris, *Science* **2010**, *327*, 662–662. DOI:10.1126/science.1184289
60. I. Shteplyuk, V. Khranovskyy, R. Yakimova, *Semicond. Sci. Technol.* **2016**, *31*, 113004. DOI:10.1088/0268-1242/31/11/113004
61. P. N. First, W. A. de Heer, T. Seyller, C. Berger, J. A. Stroscio, J.-S. Moon, *MRS Bull.* **2010**, *35*, 296–305. DOI:10.1557/mrs2010.552
62. K. V. Emtsev, A. Bostwick, K. Horn, J. Jobst, G. L. Kellogg, L. Ley, J. L. McChesney, T. Ohta, S. A. Reshanov, J. Röhr, E. Rotenberg, A. K. Schmid, D. Waldmann, H. B. Weber, T. Seyller, *Nat. Mater.* **2009**, *8*, 203–207. DOI:10.1038/nmat2382
63. C. Berger, Z. Song, X. Li, X. Wu, N. Brown, C. Naud, D. Mayou, T. Li, J. Hass, A. N. Marchenkov, E. H. Conrad, P. N. First, W. A. de Heer, *Science* **2006**, *312*, 1191–1196. DOI:10.1126/science.1125925
64. L. Talirz, H. Söde, T. Dumschlaff, S. Wang, J. R. Sanchez-Valencia, J. Liu, P. Shinde, C. A. Pignedoli, L. Liang, V. Meunier, N. C. Plumb, M. Shi, X. Feng, A. Narita, K. Müllen, R. Fasel, P.

- Ruffieux, *ACS Nano* **2017**, *11*, 1380–1388.
DOI:10.1021/acsnano.6b06405
65. G. D. Nguyen, H.-Z. Tsai, A. A. Omrani, T. Marangoni, M. Wu, D. J. Rizzo, G. F. Rodgers, R. R. Cloke, R. A. Durr, Y. Sakai, F. Liou, A. S. Aikawa, J. R. Chelikowsky, S. G. Louie, F. R. Fischer, M. F. Crommie, *Nat. Nanotechnol.* **2017**, *12*, 1077–1082. DOI:10.1038/nnano.2017.155
66. J. Cai, C. A. Pignedoli, L. Talirz, P. Ruffieux, H. Söde, L. Liang, V. Meunier, R. Berger, R. Li, X. Feng, K. Müllen, R. Fasel, *Nat. Nanotechnol.* **2014**, *9*, 896–900.
DOI:10.1038/nnano.2014.184
67. A. Celis, M. N. Nair, A. Taleb-Ibrahimi, E. H. Conrad, C. Berger, W. A. de Heer, A. Tejeda, *J. Phys. D. Appl. Phys.* **2016**, *49*, 143001. DOI:10.1088/0022-3727/49/14/143001
68. A. J. Way, R. M. Jacobberger, N. P. Guisinger, V. Saraswat, X. Zheng, A. Suresh, J. H. Dwyer, P. Gopalan, M. S. Arnold, *Nat. Commun.* **2022**, *13*, 2992.
69. J. Cai, P. Ruffieux, R. Jaafar, M. Bieri, T. Braun, S. Blankenburg, M. Muoth, A. P. Seitsonen, M. Saleh, X. Feng, K. Müllen, R. Fasel, *Nature* **2010**, *466*, 470–473.
DOI:10.1038/nature09211
70. A. Narita, X.-Y. Wang, X. Feng, K. Müllen, *Chem. Soc. Rev.* **2015**, *44*, 6616–6643. DOI:10.1039/C5CS00183H
71. Y.-C. Chen, D. G. de Oteyza, Z. Pedramrazi, C. Chen, F. R. Fischer, M. F. Crommie, *ACS Nano* **2013**, *7*, 6123–6128.
DOI:10.1021/nn401948e
72. R. S. K. Houtsmma, J. de la Rie, M. Stöhr, *Chem. Soc. Rev.* **2021**, *50*, 6541–6568. DOI:10.1039/D0CS01541E
73. H. Wang, H. S. Wang, C. Ma, L. Chen, C. Jiang, C. Chen, X. Xie, A.-P. Li, X. Wang, *Nat. Rev. Phys.* **2021**, *3*, 791–802.
DOI:10.1038/s42254-021-00370-x
74. P. H. Jacobse, A. Kimouche, T. Gebraad, M. M. Ervasti, J. M. Thijssen, P. Liljeroth, I. Swart, *Nat. Commun.* **2017**, *8*, 119.
DOI:10.1038/s41467-017-00195-2
75. Y.-C. Chen, T. Cao, C. Chen, Z. Pedramrazi, D. Haberer, D. G. de Oteyza, F. R. Fischer, S. G. Louie, M. F. Crommie, *Nat. Nanotechnol.* **2015**, *10*, 156–160.
DOI:10.1038/nnano.2014.307
76. W. Niu, S. Sopp, A. Lodi, A. Gee, F. Kong, T. Pei, P. Gehring, J. Nägele, C. S. Lau, J. Ma, J. Liu, A. Narita, J. Mol, M. Burghard, K. Müllen, Y. Mai, X. Feng, L. Bogani, *Nat. Mater.* **2023**, *22*, 180–185. DOI:10.1038/s41563-022-01460-6
77. J. Wu, W. Pisula, K. Müllen, *Chem. Rev.* **2007**, *107*, 718–747.
DOI:10.1021/cr068010r
78. A. Narita, X. Feng, K. Müllen, *Chem. Rec.* **2015**, *15*, 295–309.
DOI:10.1002/tcr.201402082
79. M. Koch, F. Ample, C. Joachim, L. Grill, *Nat. Nanotechnol.* **2012**, *7*, 713–717. DOI:10.1038/nnano.2012.169
80. D. J. Rizzo, G. Veber, T. Cao, C. Bronner, T. Chen, F. Zhao, H. Rodriguez, S. G. Louie, M. F. Crommie, F. R. Fischer, *Nature* **2018**, *560*, 204–208. DOI:10.1038/s41586-018-0376-8
81. O. Gröning, S. Wang, X. Yao, C. A. Pignedoli, G. Borin Barin, C. Daniels, A. Cupo, V. Meunier, X. Feng, A. Narita, K. Müllen, P. Ruffieux, R. Fasel, *Nature* **2018**, *560*, 209–213.
DOI:10.1038/s41586-018-0375-9
82. L. Talirz, P. Ruffieux, R. Fasel, *Adv. Mater.* **2016**, *28*, 6222–6231. DOI:10.1002/adma.201505738
83. P. H. Jacobse, M. J. J. Mangnus, S. J. M. Zevenhuizen, I. Swart, *ACS Nano* **2018**, *12*, 7048–7056.
DOI:10.1021/acsnano.8b02770
84. S. Kawai, S. Nakatsuka, T. Hatakeyama, R. Pawlak, T. Meier, J. Tracey, E. Meyer, A. S. Foster, *Sci. Adv.* **2018**, *4*.
DOI:10.1126/sciadv.aar7181
85. X. Zhang, O. V. Yazyev, J. Feng, L. Xie, C. Tao, Y.-C. Chen, L. Jiao, Z. Pedramrazi, A. Zettl, S. G. Louie, H. Dai, M. F. Crommie, *ACS Nano* **2013**, *7*, 198–202. DOI:10.1021/nn303730v
86. J. Lawrence, A. Berdonces-Layunta, S. Edalatmanesh, J. Castro-Esteban, T. Wang, A. Jimenez-Martin, B. de la Torre, R. Castrillo-Bodero, P. Angulo-Portugal, M. S. G. Mohammed, A. Matěj, M. Vilas-Varela, F. Schiller, M. Corso, P. Jelinek, D. Peña, D. G. de Oteyza, *Nat. Chem.* **2022**, *14*, 1451–1458.
DOI:10.1038/s41557-022-01042-8
87. V. Saraswat, R. M. Jacobberger, M. S. Arnold, *ACS Nano* **2021**, *15*, 3674–3708. DOI:10.1021/acsnano.0c07835
88. V. Saraswat, R. M. Jacobberger, M. S. Arnold, *ACS Nano* **2021**, *15*, 9194–9194. DOI:10.1021/acsnano.1c03098
89. M. Liu, R. Zhang, W. Chen, *Chem. Rev.* **2014**, *114*, 5117–5160.
DOI:10.1016/j.cyto.2014.07.121
90. J. Hou, Y. Shao, M. W. Ellis, R. B. Moore, B. Yi, *Phys. Chem. Chem. Phys.* **2011**, *13*, 15384. DOI:10.1039/c1cp21915d
91. H. Su, Y. H. Hu, *Energy Sci. Eng.* **2021**, *9*, 958–983.
DOI:10.1002/ese3.833
92. A. Ambrosi, C. K. Chua, A. Bonanni, M. Pumera, *Chem. Rev.* **2014**, *114*, 7150–7188. DOI:10.1021/cr500023c
93. H. Jin, C. Guo, X. Liu, J. Liu, A. Vasileff, Y. Jiao, Y. Zheng, S.-Z. Qiao, *Chem. Rev.* **2018**, *118*, 6337–6408.
DOI:10.1021/acs.chemrev.7b00689
94. E. Yoo, T. Okada, T. Akita, M. Kohyama, I. Honma, J. Nakamura, *J. Power Sources* **2011**, *196*, 110–115.
DOI:10.1016/j.jpowsour.2010.07.024
95. R. Kou, Y. Shao, D. Wang, M. H. Engelhard, J. H. Kwak, J. Wang, V. V. Viswanathan, C. Wang, Y. Lin, Y. Wang, I. A. Aksay, J. Liu, *Electrochem. Commun.* **2009**, *11*, 954–957.
DOI:10.1016/j.elecom.2009.02.033
96. L. Pavko, M. Gatalo, M. Finšgar, F. Ruiz-Zepeda, K. Eहेlebe, P. Kaiser, M. Geuß, T. Đukić, A. K. Surca, M. Šala, M. Bele, S. Cherevko, B. Genorio, N. Hodnik, M. Gaberšček, *ACS Catal.* **2022**, *12*, 9540–9548. DOI:10.1021/acscatal.2c01753
97. L. Pavko, M. Gatalo, T. Đukić, F. Ruiz-Zepeda, A. K. Surca, M. Šala, N. Maselj, P. Jovanović, M. Bele, M. Finšgar, B. Genorio, N. Hodnik, M. Gaberšček, *Carbon* **2023**, *215*, 118458.
DOI:10.1016/j.carbon.2023.118458
98. C. Lamy, E. M. Belgsir: *Handbook of Fuel Cells*, Wiley-VCH, Weinheim, Germany, **2010**.
99. A. L. Dicks, D. A. J. Rand: *Fuel Cell Systems Explained*, Wiley-VCH, Weinheim, Germany, **2018**.
DOI:10.1002/9781118706992
100. S. Wolf, M. Roschger, B. Genorio, N. Hodnik, M. Gatalo, F. Ruiz-Zepeda, V. Hacker, *J. Electrochem. Sci. Eng.* **2023**, *13*, 771–782. DOI:10.1126/sciadv.1500564
101. J. Zhang, Z. Xia, L. Dai, *Sci. Adv.* **2015**, *1*.
102. D. Deng, K. S. Novoselov, Q. Fu, N. Zheng, Z. Tian, X. Bao,

- Nat. Nanotechnol.* **2016**, *11*, 218–230.
DOI:10.1038/nnano.2015.340
103. X. Chia, M. Pumera, *Nat. Catal.* **2018**, *1*, 909–921.
DOI:10.1038/s41929-018-0181-7
104. F. Bonaccorso, L. Colombo, G. Yu, M. Stoller, V. Tozzini, A. C. Ferrari, R. S. Ruoff, V. Pellegrini, *Science* **2015**, *347*.
DOI:10.1126/science.1246501
105. Y. Li, W. Zhou, H. Wang, L. Xie, Y. Liang, F. Wei, J.-C. Idrobo, S. J. Pennycook, H. Dai, *Nat. Nanotechnol.* **2012**, *7*, 394–400.
DOI:10.1038/nnano.2012.72
106. J. Benson, Q. Xu, P. Wang, Y. Shen, L. Sun, T. Wang, M. Li, P. Papakonstantinou, *ACS Appl. Mater. Interfaces* **2014**, *6*, 19726–19736. DOI:10.1021/am5048202
107. Z. Zhao, L. Zhang, C.-Y. Lin, Z. Xia: *Carbon-Based Metal-Free Catalysts*, **2018**, Wiley-VCH, Weinheim, Germany, pp. 1–33. DOI:10.1002/9783527811458.vol1-ch1
108. L. Zhang, Q. Xu, J. Niu, Z. Xia, *Phys. Chem. Chem. Phys.* **2015**, *17*, 16733–16743. DOI:10.1039/C5CP02014J
109. Y. Sun, L. Silvioni, N. R. Sahraie, W. Ju, J. Li, A. Zitolo, S. Li, A. Bagger, L. Arnarson, X. Wang, T. Moeller, D. Bernsmeier, J. Rossmeis, F. Jaouen, P. Strasser, *J. Am. Chem. Soc.* **2019**, *141*, 12372–12381. DOI:10.1021/jacs.9b05576
110. J. Shui, M. Wang, F. Du, L. Dai, *Sci. Adv.* **2023**, *1*, e1400129.
111. W. Chen, C. Ge, J. T. Li, J. L. Beckham, Z. Yuan, K. M. Wyss, P. A. Advincula, L. Eddy, C. Kittrell, J. Chen, D. X. Luong, R. A. Carter, J. M. Tour, *ACS Nano* **2022**, *16*, 6646–6656.
DOI:10.1021/acsnano.2c01136
112. S. Wang, L. Zhang, Z. Xia, A. Roy, D. W. Chang, J.-B. Baek, L. Dai, *Angew. Chem. Int. Ed.* **2012**, *51*, 4209–4212.
DOI:10.1002/anie.201109257
113. I.-Y. Jeon, H.-J. Choi, M. Choi, J.-M. Seo, S.-M. Jung, M.-J. Kim, S. Zhang, L. Zhang, Z. Xia, L. Dai, N. Park, J.-B. Baek, *Sci. Rep.* **2013**, *3*, 1810.
114. L. Zhang, J. Niu, M. Li, Z. Xia, *J. Phys. Chem. C* **2014**, *118*, 3545–3553. DOI:10.1021/jp410501u
115. C. Su, M. Acik, K. Takai, J. Lu, S. Hao, Y. Zheng, P. Wu, Q. Bao, T. Enoki, Y. J. Chabal, K. Ping Loh, *Nat. Commun.* **2012**, *3*, 1298.
116. Y. Zheng, Y. Jiao, Y. Zhu, L. H. Li, Y. Han, Y. Chen, A. Du, M. Jaroniec, S. Z. Qiao, *Nat. Commun.* **2014**, *5*, 3783.
DOI:10.1038/ncomms4783
117. J. Wan, Z. Zhao, H. Shang, B. Peng, W. Chen, J. Pei, L. Zheng, J. Dong, R. Cao, R. Sarangi, Z. Jiang, D. Zhou, Z. Zhuang, J. Zhang, D. Wang, Y. Li, *J. Am. Chem. Soc.* **2020**, *142*, 8431–8439. DOI:10.1021/jacs.0c02229
118. L. Qu, Y. Liu, J.-B. Baek, L. Dai, *ACS Nano* **2010**, *4*, 1321–1326. DOI:10.1021/nn901850u
119. L. Dai (Ed.): *Carbon-Based Metal-Free Catalysts*, Wiley-VCH, Weinheim, Germany, **2018**.
DOI:10.1002/9783527811458
120. D. Guo, R. Shibuya, C. Akiba, S. Saji, T. Kondo, J. Nakamura, *Science* **2016**, *351*, 361–365. DOI:10.1126/science.aad0832
121. M. Nosan, L. Pavko, M. Finšgar, M. Kolar, B. Genorio, *ACS Appl. Energy Mater.* **2022**, *5*, 9571–9580.
DOI:10.1021/acsaem.2c01184
122. J. Durst, A. Siebel, C. Simon, F. Hasché, J. Herranz, H. A. Gasteiger, *Energy Environ. Sci.* **2014**, *7*, 2255–2260.
DOI:10.1039/C4EE00440J
123. J. K. Nørskov, T. Bligaard, A. Logadottir, J. R. Kitchin, J. G. Chen, S. Pandalov, U. Stimming, *J. Electrochem. Soc.* **2005**, *152*, J23. DOI:10.1149/1.1856988
124. A. Lasia: *Handbook of Fuel Cells*, Wiley-VCH, Weinheim, Germany, **2010**.
125. H. N. Nong, L. J. Falling, A. Bergmann, M. Klingenhof, H. P. Tran, C. Spöri, R. Mom, J. Timoshenko, G. Zichittella, A. Knop-Gericke, S. Piccinin, J. Pérez-Ramírez, B. R. Cuenya, R. Schlögl, P. Strasser, D. Teschner, T. E. Jones, *Nature* **2020**, *587*, 408–413. DOI:10.1038/s41586-020-2908-2
126. A. E. Thorarinsdottir, S. S. Veroneau, D. G. Nocera, *Nat. Commun.* **2022**, *13*, 1243.
DOI:10.1038/s41467-022-28723-9
127. D. Liu, X. Li, S. Chen, H. Yan, C. Wang, C. Wu, Y. A. Haleem, S. Duan, J. Lu, B. Ge, P. M. Ajayan, Y. Luo, J. Jiang, L. Song, *Nat. Energy* **2019**, *4*, 512–518.
DOI:10.1038/s41560-019-0402-6
128. Y. Zheng, Y. Jiao, A. Vasileff, S. Qiao, *Angew. Chem. Int. Ed.* **2018**, *57*, 7568–7579. DOI:10.1002/anie.201710556
129. N. Dubouis, A. Grimaud, *Chem. Sci.* **2019**, *10*, 9165–9181.
DOI:10.1039/C9SC03831K
130. A. Grimaud, O. Diaz-Morales, B. Han, W. T. Hong, Y.-L. Lee, L. Giordano, K. A. Stoerzinger, M. T. M. Koper, Y. Shao-Horn, *Nat. Chem.* **2017**, *9*, 457–465.
DOI:10.1038/nchem.2695
131. J. Herranz, J. Durst, E. Fabbri, A. Patru, X. Cheng, A. A. Permyakova, T. J. Schmidt, *Nano Energy* **2016**, *29*, 4–28.
DOI:10.1016/j.nanoen.2016.01.027
132. R. Subbaraman, D. Tripkovic, D. Strmcnik, K.-C. Chang, M. Uchimura, A. P. Paulikas, V. Stamenkovic, N. M. Markovic, *Science* **2011**, *334*, 1256–1260.
DOI:10.1126/science.1211934
133. D. Strmcnik, P. P. Lopes, B. Genorio, V. R. Stamenkovic, N. M. Markovic, *Nano Energy* **2016**, *29*, 29–36.
DOI:10.1016/j.nanoen.2016.04.017
134. P. P. Lopes, D. Y. Chung, X. Rui, H. Zheng, H. He, P. Farinazzo Bergamo Dias Martins, D. Strmcnik, V. R. Stamenkovic, P. Zapol, J. F. Mitchell, R. F. Klie, N. M. Markovic, *J. Am. Chem. Soc.* **2021**, *143*, 2741–2750.
DOI:10.1021/jacs.0c08959
135. D. Y. Chung, P. P. Lopes, P. Farinazzo Bergamo Dias Martins, H. He, T. Kawaguchi, P. Zapol, H. You, D. Tripkovic, D. Strmcnik, Y. Zhu, S. Seifert, S. Lee, V. R. Stamenkovic, N. M. Markovic, *Nat. Energy* **2020**, *5*, 222–230.
DOI:10.1038/s41560-020-0576-y
136. J. Suntivich, K. J. May, H. A. Gasteiger, J. B. Goodenough, Y. Shao-Horn, *Science* **2011**, *334*, 1383–1385.
DOI:10.1126/science.1212858
137. Y. Zheng, Y. Jiao, Y. Zhu, L. H. Li, Y. Han, Y. Chen, A. Du, M. Jaroniec, S. Z. Qiao, *Nat. Commun.* **2014**, *5*, 3783.
DOI:10.1038/ncomms4783
138. Y. Jiao, Y. Zheng, K. Davey, S.-Z. Qiao, *Nat. Energy* **2016**, *1*, 16130. DOI:10.1038/nenergy.2016.130
139. Y. Zhao, R. Nakamura, K. Kamiya, S. Nakanishi, K. Hashi-

- moto, *Nat. Commun.* **2013**, *4*, 2390.
DOI:10.1038/ncomms3390
140. R. Czerw, M. Terrones, J.-C. Charlier, X. Blase, B. Foley, R. Kamalakaran, N. Grobert, H. Terrones, D. Tekleab, P. M. Ajayan, W. Blau, M. Rühle, D. L. Carroll, *Nano Lett.* **2001**, *1*, 457–460. DOI:10.1021/nl015549q
141. Z. Hou, X. Wang, T. Ikeda, K. Terakura, M. Oshima, M. Kakimoto, *Phys. Rev. B* **2013**, *87*, 165401.
DOI:10.1103/PhysRevB.87.165401
142. S. Chen, J. Duan, M. Jaroniec, S. Qiao, *Adv. Mater.* **2014**, *26*, 2925–2930. DOI:10.1002/adma.201305608
143. T. Y. Ma, S. Dai, M. Jaroniec, S. Z. Qiao, *Angew. Chem. Int. Ed.* **2014**, *53*, 7281–7285. DOI:10.1002/anie.201403946
144. K. Lee, J. Lim, M. J. Lee, K. Ryu, H. Lee, J. Y. Kim, H. Ju, H.-S. Cho, B.-H. Kim, M. C. Hatzell, J. Kang, S. W. Lee, *Energy Environ. Sci.* **2022**, *15*, 2858–2866.
DOI:10.1039/D2EE00548D
145. R. Orrù, R. Licheri, A. M. Locci, A. Cincotti, G. Cao, *Mater. Sci. Eng. R Rep.* **2009**, *63*, 127–287.
DOI:10.1016/j.mser.2008.09.003
146. S. Grasso, Y. Sakka, G. Maizza, *Sci. Technol. Adv. Mater.* **2009**, *10*, 053001. DOI:10.1088/1468-6996/10/5/053001
147. K. M. Wyss, Z. Wang, L. B. Alemany, C. Kittrell, J. M. Tour, *ACS Nano* **2021**, *15*, 10542–10552.
DOI:10.1021/acsnano.1c03197
148. K. M. Wyss, J. L. Beckham, W. Chen, D. X. Luong, P. Hundi, S. Raghuraman, R. Shahsavari, J. M. Tour, *Carbon* **2021**, *174*, 430–438. DOI:10.1016/j.carbon.2020.12.063
149. B. I. Jakobson, J. M. Tour, M. G. Stanford, K. V. Bets, D. X. Luong, P. A. Advincula, W. Chen, J. T. Li, Z. Wang, E. A. McHugh, W. A. Algozeeb, *ACS Nano* **2020**, *14*, 13691–13699.
DOI:10.1021/acsnano.0c05900
150. P. A. Advincula, D. X. Luong, W. Chen, S. Raghuraman, R. Shahsavari, J. M. Tour, *Carbon* **2021**, *178*, 649–656.
DOI:10.1016/j.carbon.2021.03.020
151. E. Benhelal, G. Zahedi, E. Shamsaei, A. Bahadori, *J. Clean Prod.* **2013**, *51*, 142–161. DOI:10.1016/j.jclepro.2012.10.049
152. A. Cantini, L. Leoni, F. De Carlo, M. Salvio, C. Martini, F. Martini, *Sustainability* **2021**, *13*, 3810.
DOI:10.3390/su13073810
153. P. A. Advincula, W. Meng, L. J. Eddy, J. L. Beckham, I. R. Siqueira, D. X. Luong, W. Chen, M. Pasquali, S. Nagarajiah, J. M. Tour, *Macromol. Mater. Eng.* **2023**, *308*, 2200640.
DOI:10.1002/mame.202200640
154. J. Y. Huang, S. Chen, Z. F. Ren, G. Chen, M. S. Dresselhaus, *Nano Lett.* **2006**, *6*, 1699–1705.
DOI:10.1021/nl0609910
155. X. Liu, L. Dai, *Nat. Rev. Mater.* **2016**, *1*, 16064.
DOI:10.1038/natrevmats.2016.64
156. K. M. Wyss, W. Chen, J. L. Beckham, P. E. Savas, J. M. Tour, *ACS Nano* **2022**.
157. X. Wang, G. Sun, P. Routh, D.-H. Kim, W. Huang, P. Chen, *Chem. Soc. Rev.* **2014**, *43*, 7067–7098.
DOI:10.1039/C4CS00141A
158. S. Dong, Y. Song, M. Su, G. Wang, *J. Chem. Eng.* **2024**, *481*, 147988. DOI:10.1016/j.cej.2023.147988
159. S. Dong, Y. Song, K. Ye, J. Yan, G. Wang, *EcoMat* **2022**, *4*, 12212. DOI:10.1002/eom2.12212
160. W. Chen, R. Salvatierra, J. Li, C. Kittrell, J. Beckham, *Adv. Mater.* **2023**, *8*, 2207303.
161. K. Wyss, D. Luong, J. Tour, *Adv. Mater.* **2022**, *8*, 2106970.
162. X. Zhu, L. Lin, M. Pang, M. Nat. Commun. **2024**, *15*, 3218.
DOI:10.1038/s41467-024-48591-9
163. W. Chen, J. Chen, K. Bets, R. Salvatierra, K. Wyss, *Sci. Adv.* **2023**, *9*, 5131. DOI:10.1126/sciadv.adh5131

Povzetek

Naraščajoče povpraševanje po trajnostnih in učinkovitih tehnologijah za pretvorbo energije zahteva stalno raziskovanje novih materialov in metod. Metoda Flash Joule (FJH) se pojavlja kot obetavna tehnika za množično proizvodnjo grafena, saj ponuja prednosti pred tradicionalnimi metodami. FJH hitro segreje ogljikove prekurzorje do ekstremnih temperatur z uporabo visokih električnih tokov, pri čemer se po hitrem ohlajanju tvori bliskoviti grafen. Ta pristop omogoča hitro obdelavo, visoko zmogljivost in uporabo različnih ogljikovih virov, vključno z biomaso in odpadki, kar ga naredi trajnostnega in stroškovno učinkovitega. Poleg tega ustvarja minimalne odpadke in proizvaja bliskoviti grafen z izboljšano prevodnostjo, kar je ključnega pomena za energetske aplikacije. Zaradi možnosti razširitve, vsestranskosti in učinkovitosti se FJH postavlja kot ključna metoda za komercializacijo grafena v različnih industrijah, zlasti pri pretvorbi energije. Ta pregled celovito obravnava principe sinteze FJH, s poudarkom na učinkovitosti, razširljivosti in trajnosti. Poleg tega analizira nedavne napredke pri elektrokatalizatorjih, temelječih na bliskovitem grafenu, in raziskuje njihov vpliv na obnovljivo energijo ter trajnostno elektrokatalizo. Obravnavani so izzivi in priložnosti, pri čemer so načrtane smernice za prihodnje raziskave. Nadaljnji napredek ima velik potencial za revolucijo v proizvodnji grafena in njegovo vključitev v energetske sisteme nove generacije, kar bo prispevalo k prehodu na čistejšo energetske rešitve.



Except when otherwise noted, articles in this journal are published under the terms and conditions of the Creative Commons Attribution 4.0 International License